Sustained Stabilization of the Resistive-Wall Mode by Plasma Rotation in the DIII-D Tokamak

A. M. Garofalo,* E. J. Strait, L. C. Johnson,† R. J. La Haye, E. A. Lazarus,‡ G. A. Navratil,* M. Okabayashi,† J. T. Scoville, T. S. Taylor, and A. D. Turnbull

General Atomics, P.O. Box 85608, San Diego, California 92186-5608

(Received 7 November 2001; published 15 November 2002)

Values of the normalized plasma pressure up to twice the free-boundary stability limit predicted by ideal magnetohydrodynamic (MHD) theory have been sustained in the DIII-D tokamak. Long-wavelength modes are stabilized by the resistive wall and rapid plasma toroidal rotation. High rotation speed is maintained by minimization of nonaxisymmetric magnetic fields, overcoming a long-standing impediment [E. J. Strait *et al.*, Phys. Rev. Lett. **74**, 2483 (1995)]. The ideal-MHD pressure limit calculated with an ideal wall is observed as the operational limit to the normalized plasma pressure.

DOI: 10.1103/PhysRevLett.89.235001 PACS numbers: 52.55.Fa, 52.30.–q, 52.55.Tn, 52.65.Kj

The long time-scale stabilization of a hot plasma by a resistive wall is an important test of magnetohydrodynamic (MHD) theory. It is also a problem of great practical significance for controlled nuclear fusion research. Standard ideal-MHD theory predicts that the long-wavelength (toroidal mode number $n = 1$) "kink" modes will limit the achievable β in tokamaks and other toroidal magnetic confinement devices. [Here $\beta = \langle p \rangle / (B^2/2\mu_0)$ is the dimensionless plasma pressure, with B the magnetic field strength.] A perfectly conducting wall close to the plasma is predicted to stabilize the kink mode, thus raising the maximum β significantly above the free-boundary or no-wall limit. However, since real walls have finite conductivity, the kink mode is instead converted to a resistive wall mode (RWM), i.e., a mode having a growth time of the order of the decay time of the eddy currents in the resistive wall, τ_w [1].

Modifications to the ideal-MHD theory that introduce some mechanism for dissipation in the plasma allow for energy and momentum exchange between the rotating fluid and the nearly stationary RWM. With plasma rotation speed above a threshold that depends in part on the nature of the dissipation, the RWM can be stabilized [2,3]. Thus, a resistive wall close to the plasma in combination with plasma dissipation and plasma rotation are predicted to raise the maximum β up to the ideal-wall limit, i.e., the β limit which can be calculated with a perfectly conducting wall in place of the resistive wall.

Previous experiments have achieved plasma stability at β exceeding the no-wall limit for times long compared to both τ_w (~ 5 ms) and the energy confinement time, τ_E (~ 150 ms), demonstrating that stabilization by the resistive wall and plasma rotation was achieved. Still, the stabilization in those experiments had a transient character, because the plasma rotation always decreased whenever β exceeded the calculated no-wall limit, eventually leading to a rollover or collapse of the confined pressure [4,5].

The key to understanding the loss of rotation at β above the no-wall stability limit has been the discovery that small static asymmetries in the magnetic field (magnetic error fields) can resonantly excite stable RWMs as the plasma approaches marginal stability, leading to enhanced drag on the rotating fluid. The correction of $n = 1$ magnetic error fields therefore becomes crucial as β exceeds the no-wall limit. In the experiments reported here, the optimal configuration of applied correction fields has been determined equivalently using two independent techniques.

Sustained stabilization of the RWM by plasma rotation was obtained reproducibly in discharges with optimal correction of the $n = 1$ error field, and a moderate increase in the angular momentum injection over previous experiments (Fig. 1). Here we use the normalized β, $\beta_N = \beta/(I_p/aB)$, as a measure of the plasma pressure (I_p is the toroidal plasma current, a is the plasma minor radius) since the no-wall ideal-MHD stability limit can be simply expressed as $\beta_N^{\text{no-wall}} \approx \lambda \ell_i$. The plasma internal inductance, ℓ_i, is a measure of the peakedness of the radial profile of the toroidal current density; the value of λ depends on details of the internal distribution of pressure and magnetic field, and in these plasmas is calculated to be $\lambda \sim 2.4$. In discharge 107603, β_N is maintained $\geq 50\%$ above the $n = 1$ no-wall limit for up to ≥ 1.5 s, or about 300 times the wall time constant, τ_w and 10 times the energy confinement time, τ_E. The high-β phase is terminated by one of the power supplies for the plasma shaping coils reaching its current limit.

Figure 1 also shows time traces for two discharges with nonoptimal correction of the magnetic error fields (106520, 106530). Correction of the $n = 1$ magnetic error field is done on DIII-D with a set of six external coils at the outer midplane, the C-coil [6]. The current in one pair of these coils is shown for reference in Fig. 1(c). The time trace of the angular momentum confinement time, τ_L, is shown in Fig. 1(b). In all the discharges τ_L at first increases rapidly as the neutral beam heating power is stepped up, and a transition from low (L) to high (H) confinement is triggered at $t \sim 1100$ ms. Subsequently, the evolution of τ_L is very different for discharges

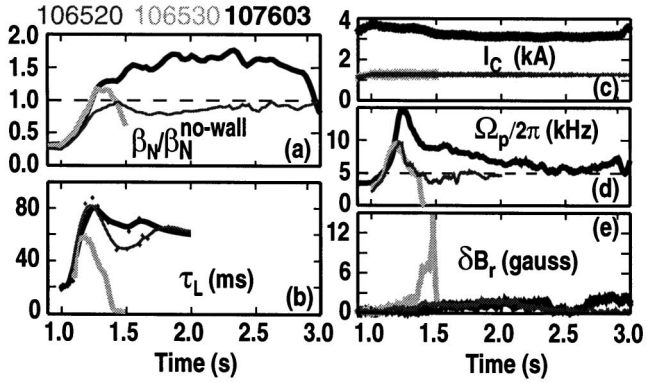

FIG. 1. Time history of discharges at low β (106520) and high β (106530) with some residual error field, and high β with optimized error correction (107603). (a) Ratio of normalized β to calculated no-wall limit, (b) angular momentum confinement time, (c) error correction current in one of the C-coil pairs, (d) plasma toroidal rotation at about the radius of $q = 2$ surface, and (e) amplitude of the radial magnetic field of the $n = 1$ RWM measured at the outer midplane. Major radius $R_0 = 1.8$ m, minor radius $a = 0.6$ m, and toroidal field $B_T = 2.1$ T.

106520 and 106530, despite the similar, nonoptimal error correction current. The difference shown is typical between discharges that exceed and do not exceed the no-wall β limit (with nonoptimal error correction). For discharge 106530, as β_N approaches and then exceeds $\beta_N^{\text{no-wall}}$, τ_L shows a strong inversion of trend, plunging towards zero. At this time the plasma rotation Ω_p, observed from Doppler shifted impurity radiation, decreases rapidly until the RWM becomes unstable. We have found for these plasmas that the threshold rotation measured at the flux surface with safety factor value $q = 2$ is within 50% of the value predicted by Ref. [2] for stabilization of the RWM. The measured value of $\sim$5 kHz is approximately 3% of the toroidal Alfvén frequency $f_A = V_A/2\pi Rq$ (V_A is the Alfvén speed) or 30% of the toroidal sound frequency $f_S = V_S/2\pi Rq$ (V_S is the sound speed). When the plasma rotation decreases below the threshold in this discharge with β_N above $\beta_N^{\text{no-wall}}$, the $n = 1$ RWM grows and causes a β collapse ($t = 1350$ ms).

The strong damping of rotation is a consequence of β_N exceeding $\beta_N^{\text{no-wall}}$. In discharge 106520, which remains below the no-wall limit, τ_L is significantly higher than in discharge 106530 despite the similar error field. Note that when $\Omega_p/2\pi$ decreases below $\sim$5 kHz in the lower-β discharge, the RWM remains stable.

The optimization of the error field correction removes the decay of τ_L observed when β_N exceeds $\beta_N^{\text{no-wall}}$, as shown by the evolution of τ_L for discharge 107603. Here, with optimal correction of the $n = 1$ error field, τ_L remains high though β_N approaches, and then significantly exceeds, $\beta_N^{\text{no-wall}}$. The plasma rotation in discharge 107603 is higher than in other cases because of simultaneous high τ_L and higher power and momentum from neutral beam injection. Since $\Omega_p/2\pi$ is sustained above $\sim$5 kHz, the RWM remains stable even with β_N well above $\beta_N^{\text{no-wall}}$.

It was suggested by Boozer [7] that the reduction in τ_L when β_N exceeds $\beta_N^{\text{no-wall}}$ could be explained as the result of an effective "amplification" by the plasma of the intrinsic error field which is resonant with the rotationally stabilized RWM. Asymmetries in the magnetic field can exert drag on Ω_p at the singular surfaces, in a similar way to the behavior of "slipping" in an induction motor [8,9]. Dedicated experiments [10,11] have indeed confirmed that above $\beta_N^{\text{no-wall}}$, a RWM which is stabilized by plasma rotation can be driven to a finite amplitude by a resonant, static magnetic field perturbation applied externally. The stable RWM amplitude can be several times larger than the amplitude of the external perturbation at the resonant surface, and is observed to increase with increasing β_N.

Two independent methods were used to find the optimal error field correction. One method is based on plasma rotation, the other on measurements of the magnetic field asymmetry itself. In the first method, the optimum $n = 1$ correction field in discharges with $\beta_N > \beta_N^{\text{no-wall}}$ is determined by changing shot-by-shot the field applied by the C-coil, until the rotation decay rate during the high-β phase is minimized [12].

The second method exploits the increase in the resonant plasma response to the intrinsic field asymmetry as β increases above the no-wall limit (error field amplification) [11]. This change in the magnetic asymmetry is used as input for the DIII-D RWM feedback system [10,13], which is then able to drive the appropriate correction currents in the C-coil. Potentially, the feedback method avoids the need for explicit measurements of the field asymmetries.

Remarkably, the two methods converge to the same error correction field. In Fig. 2 the amplitude and phase of the $n = 1$ correction field from the C-coil are compared for two discharges. Discharge 107603 used correction currents optimized with respect to plasma rotation, while in discharge 106532 the correction is obtained through use of the RWM feedback. The correction current amplitude and phase are quite similar for the two discharges, and the plasma performance is nearly the same. The agreement of the two methods supports the hypothesis that error field amplification is responsible for the reduction of Ω_p at β_N above $\beta_N^{\text{no-wall}}$.

Detailed stability calculations confirm that the stability limit in absence of a wall is well approximated by $\beta_N^{\text{no-wall}} = 2.4\ell_i$. Results of several tests of the time dependence of $\beta_N^{\text{no-wall}}$ are shown in Fig. 3. The plasma equilibrium was numerically reconstructed at several times throughout the high-β phase of discharge 106535 [solid black curve in Fig. 3(b)]. Ideal-MHD stability analysis using the GATO code [14] shows that in the absence of a resistive wall and of plasma rotation, the $n = 1$ kink mode would be unstable when β_N exceeds a value $= 2.4\ell_i$ at $t \sim 1200$ ms [triangles in Fig. 3(a)], consistent with previous calculations in similar

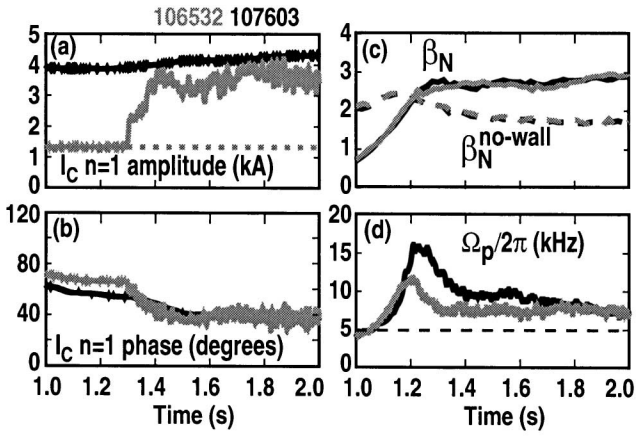

FIG. 2. Comparison of the amplitude (a) and toroidal phase (b) of the C-coil currents in discharges 106532 and 107603, and their effects on normalized β (c) and plasma rotation (d). Correction currents are determined by shot-to-shot minimization of the plasma rotation decay rate in discharge 107603 (black) and by RWM feedback using internal poloidal field probes as sensors in discharge 106532 (gray).

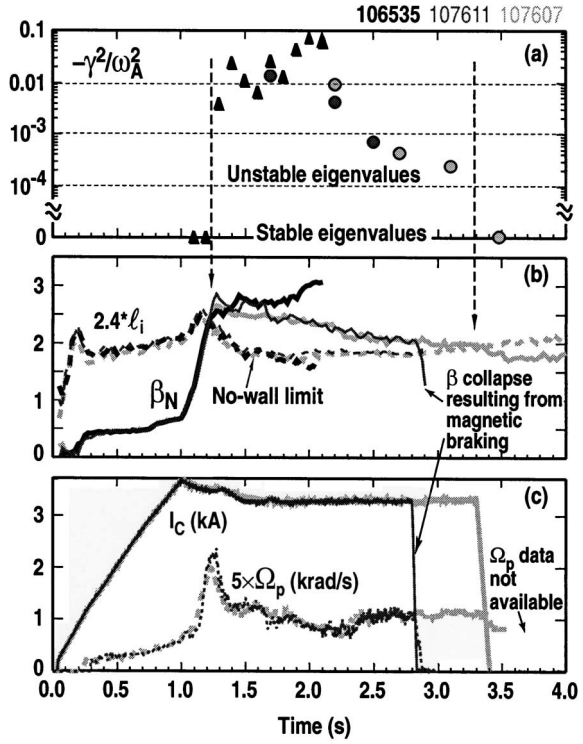

FIG. 3. Numerical and experimental tests of the time evolution of the no-wall β_N limit. (a) Square of the $n = 1$ mode growth rate normalized to the Alfvén frequency calculated with GATO without a wall for similar discharges (black triangles for 106535, light and dark circles for 107607 and 107611). Positive values of the ordinate indicate instability. The ordinate axis is shown with a break to include zero (stable) eigenvalues. The predicted growth rate crosses the stability boundary when (b) β_N crosses the approximate no-wall limit $= 2.4\ell_i$, indicated by vertical dashed arrows. (c) Magnetic braking of the plasma rotation Ω_p, obtained by turning off the error field correction current I_c, leads to RWM onset and β collapse only when β_N exceeds $2.4\ell_i$ (dark gray).

discharges [5]. At this time the plasma has just transitioned from low (L) to high (H) confinement mode, and ℓ_i is decreasing rapidly. Stability calculations for similar discharges where β_N is allowed to decrease slowly below $2.4\ell_i$ [solid gray curves in Fig. 3(b)] show that the marginal stability boundary of $2.4\ell_i$ is maintained also at later times [circles in Fig. 3(a)].

Figure 3 also shows the result of an experimental test of the no-wall limit calculation for these two discharges, using magnetic braking of Ω_p [9]. In discharge 107607 the correction coil current is turned off when β_N has just decreased below the predicted $\beta_N^{\text{no-wall}}$. The increased magnetic field asymmetry causes Ω_p to decrease to a level where a new torque equilibrium is established, and the plasma survives at constant β. In discharge 107611, the correction coil is turned off when β_N is just above the predicted $\beta_N^{\text{no-wall}}$. Here the drag on Ω_p is amplified by the rotationally stabilized, resonant RWM. When Ω_p drops below a critical value, the RWM becomes unstable and grows, causing a β collapse. Such macroscopic comparisons between experiment and modeling provide a demonstration of the remarkable accuracy (within 10% in β_N) of the ideal-MHD calculations of the no-wall stability limit.

In discharge 106535, β_N reaches twice the value of $\beta_N^{\text{no-wall}}$ [Fig. 3(b)], at which point ($t \sim 2100$ ms) the plasma disrupts due to a rapidly growing instability. The instability is consistent with an $n = 1$ kink mode occurring at the stability limit calculated with an ideal wall. Just before the instability, data from the toroidal array of Mirnov loops [Figs. 4(a)–4(c)] show an $n = 1$ structure with a rotation frequency $\omega/2\pi = 1$ kHz and a growth time of $\tau_g \sim 0.3$ ms. Usually, an RWM is expected to have a growth time comparable to τ_w and a rotation rate comparable to $1/\tau_w$, while here the observed growth and rotation are an order of magnitude faster. The relatively rapid mode rotation and growth suggest that this instability would behave about the same in the presence of a perfectly conducting wall. We carried out ideal-MHD calculations of the $n = 1$ stability with an ideal wall approximating closely the shape of the DIII-D vessel. The stability code allows us to vary the minor radius of the ideal wall, to test the effect of plasma-wall separation on the instability. As shown in Fig. 4(d), the plasma at $t = 2040$ ms is calculated to be stable with the ideal wall at the position of the vacuum vessel. Variation of the equilibrium reconstruction shows that with only a slightly higher β_N ($< 10\%$, consistent with experimental uncertainties), the equilibrium becomes unstable with the ideal wall at the position of the vacuum vessel. The calculations therefore suggest that ~60 ms before the instability, the experimental equilibrium is very close to the stability limit with respect to wall position and also with respect to β_N.

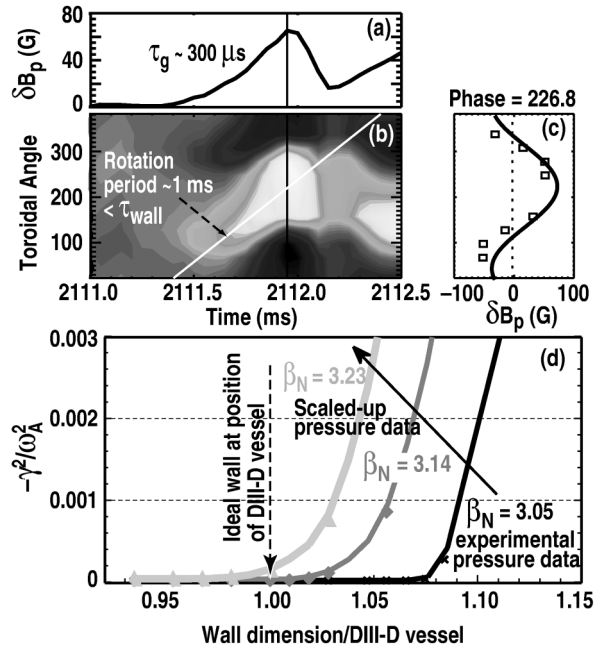

FIG. 4. Magnetic measurements of the fast growing $n = 1$ MHD instability in discharge 106535 at $\beta_N \approx 2\beta_N^{\text{no-wall}}$. (a) Time trace of the $n = 1$ amplitude obtained from a midplane array of Mirnov probes. (b) Contour plot of all the Mirnov probe signals vs time and toroidal angle. (c) Same signals vs toroidal angle at time of peak amplitude. (d) Calculated growth rate of the $n = 1$ kink mode vs assumed position of a perfectly conducting wall for equilibrium reconstructions at ~60 ms before the instability. Reconstructions are calculated using the experimental pressure profile (black curve), or with the measured pressure profile scaled up by ~3% (dark gray) and by ~6% (light gray).

The measured growth time is consistent with calculations of the RWM growth rate at β_N near the ideal-wall limit performed with the electromagnetics code VALEN [15], which uses a detailed model of the DIII-D resistive vessel and the $n = 1$ kink eigenfunction predicted by GATO. The growth time can also be explained by a model [16] for an ideal mode slowly driven through the stability boundary: $\tau_g = \tau_{\text{MHD}}^{2/3}\tau_h^{1/3}$, where τ_{MHD} is of the order of the expected growth time of the ideal-MHD mode and τ_h is the time scale for the increase of the instability drive. For a kink-ballooning RWM, we assume the instability drive is proportional to the ratio β_N/ℓ_i. Here the measured rise time for β_N/ℓ_i before the instability is $\tau_h \sim 2$ s, and the measured growth time of the kink mode is $\tau_g = 300$ μs, which yield $\tau_{\text{MHD}} \sim 4$ μs. This time is indeed consistent with expectations for ideal-MHD instabilities. In summary, the experimentally observed growth time of ~0.3 ms could be explained either by an RWM at β_N just below the ideal-wall limit or by an ideal kink mode slowly driven through the ideal-wall limit. In both cases, the experimental observation is consistent with β_N being very close to the ideal-wall limit.

These recent DIII-D experiments demonstrate that passive stabilization of the RWM by resistive wall and plasma rotation is possible, even at β values significantly above the no-wall limit. Accurate correction of magnetic field asymmetries is critical to minimize plasma rotation decay at β above the no-wall limit. RWM feedback operation provides a new method to determine the improved magnetic field correction by sensing and opposing the resonant response of the stable RWM to the uncorrected field asymmetry. With improved magnetic field symmetry, and increased angular momentum injection, these experiments point the way to sustained operation, at plasma pressure up to twice the ideal-MHD $n = 1$ free-boundary limit. At twice the free-boundary pressure limit, an MHD instability is observed, which is consistent with having reached the "ideal wall" pressure limit predicted by stability calculations.

These experiments have removed one of the major long-standing obstacles to sustainment of wall stabilized plasmas at pressures well above the conventional limit. The implications of this work are therefore quite profound for the development of steady-state advanced tokamaks, since it may allow these devices to operate at high pressure for as long as sufficient torque is provided.

This research is sponsored by the U.S. Department of Energy under Contracts No. DE-AC03-99ER54463, No. DE-FG02-89ER53297, No. DE-AC05-00OR22725, and No. DE-AC02-76CH03073. The authors thank the DIII-D team for their support.

*Also at Columbia University, New York, NY.
Email address: garofalo@fusion.gat.com
†Also at Princeton Plasma Physics Laboratory, Princeton, NJ.
‡Also at Oak Ridge National Laboratory, Oak Ridge, TN.

[1] J. P. Freidberg, *Ideal Magnetohydrodynamics* (Plenum Press, New York, 1987).
[2] A. Bondeson and D. J. Ward, Phys. Rev. Lett. **72**, 2709 (1994).
[3] R. Betti and J. P. Freidberg, Phys. Rev. Lett. **74**, 2949 (1995).
[4] E. J. Strait *et al.*, Phys. Rev. Lett. **74**, 2483 (1995).
[5] A. M. Garofalo *et al.*, Phys. Rev. Lett. **82**, 3811 (1999).
[6] R. J. Buttery *et al.*, Nucl. Fusion **39**, 1827 (1999).
[7] A. H. Boozer, Phys. Rev. Lett. **86**, 5059 (2001).
[8] T. H. Jensen, A.W. Leonard, and A.W. Hyatt, Phys. Fluids B **5**, 1239 (1993).
[9] R. Fitzpatrick, Phys. Plasmas **5**, 3325 (1998).
[10] A. M. Garofalo *et al.*, Nucl. Fusion **41**, 1171 (2001).
[11] A. M. Garofalo *et al.*, Phys. Plasmas **9**, 1997 (2002).
[12] A. M. Garofalo *et al.*, Nucl. Fusion **42**, 1335 (2002).
[13] M. Okabayashi *et al.*, Phys. Plasmas **8**, 2071 (2001).
[14] L. C. Bernard, F. J. Helton, and R.W. Moore, Comput. Phys. Commun. **24**, 377 (1981).
[15] J. Bialek *et al.*, Phys. Plasmas **8**, 2170 (2001).
[16] J. D. Callen *et al.*, Phys. Plasmas **6**, 2963 (1999).